UNIVERSITÉ LIBRE DE BRUXELLES

BRUFACE BRUSSELS FACULTY OF ENGINEERING

VRIJE UNIVERSITEIT BRUSSEL

Channel modeling for 5G small cells

[ELEC-H415] - Communication channels

Warre De Winne

28/05/2023

Contents

1 Introduction

This report discusses the the modeling of a downlink channel of a 5G small cell base station towards a mobile receiver on the Marché aux Poissons and its connecting streets. This is done through ray tracing.

The first part of the report discusses the channel parameters and the theoretical background used to construct the model of the channel. Then the obtained results like the received power, signal-to-noise ratio, Rice factor, delay spread and channel impulse response are discussed. Finally, a propagation model is constructed by calculating the path loss and characterising the statistical fading. This is then used to determine the cell range based on the probability of connection at the cell edge.

2 Channel parameters

A short overview of the channel parameters and certain constants used in this report, are given below. Any other parameters used are defined in the report itself.

- $Carrier\, frequency:\ f_c = 27GHz$
- $height:\ h_{base\, station} = h_{recevier} = 2m$
- $EIRP = 1W$
- $relative\, permitivity:\ \epsilon_r = 3 - 5$
- $Wave\, vector:\ \beta = \frac{2\pi f_c}{c} = 565.487m$
- $Transmitter\, resistance:\ R_a = 73\Omega$

3 Theoretical Foundations: Ray Tracing

This section discusses how the induced voltage for every considered scenario is obtained. Note that diffraction is only taken into account when no line-of-sight is present.

3.1 Line-of-sight Ray

The line-of-sight electrical field at the receiver is easily calculated using following formula:

$$\vec{E}^{LOS} = \sqrt{60EIRP}\frac{e^{-j\beta d^{LOS}}}{d^{LOS}}\vec{1_\theta} \tag{1}$$

Where EIRP is equal to $P_{Tx} * G_{Tx}$ and d^{LOS} the distance between the base station and the receiver.

The effective height of a vertical half-wave dipole antenna is equal to

$$\vec{h_e}(\theta,\phi) = -\frac{\lambda}{\pi}\frac{cos(\frac{\pi}{2}cos(\theta))}{sin^2\theta}\vec{1_a} = -0.0035\vec{1_z} \tag{2}$$

Since θ is equal to $\pi/2$ and $\lambda = c/f_c = 0.0111$ m. With c the speed of light and f_c the carrier frequency equal to $27 * 10^9$ Hz.

multiplying the electrical field and the effective height leads to the open circuit voltage and is equal to:

$$\begin{aligned} V_{oc}^{LOS} &= \vec{E}^{LOS} * \vec{h_e}(\theta,\phi) \\ &= -0.0035\sqrt{60EIRP}\frac{e^{-j\beta d^{LOS}}}{d^{LOS}}sin(\theta) \\ &= -0.0035\sqrt{60EIRP}\frac{e^{-j\beta d^{LOS}}}{d^{LOS}} \end{aligned} \tag{3}$$

Since θ is equal to $\frac{\pi}{2}$.

3.2 Ground Reflection

Calculating the open circuit voltage of a ground reflection ray is similar to that of a line-of-sight ray. The only thing that changes is the effective height, an extra reflection factor and the distance between the base station and receiver. The electrical field is equal to

$$\vec{E}^{GROUND} = \Gamma_{\parallel}\sqrt{60EIRP}\frac{e^{-j\beta d^{GROUND}}}{d^{GROUND}}\vec{1_\theta} \tag{4}$$

The distance d^{GROUND} is calculated using the property that the receiver and base station are at the same height. Thus the reflected ray between the ground and the receiver has the same length as the ray from the base station to the ground. Using this property and the Pythagoras theorem, one obtains

$$d^{GROUND} = \sqrt{(d^{LOS})^2 + (2h_{bs})^2} \tag{5}$$

With h_{bs} the height of the base station, here equal to 2 meter. This formula proves useful since d^{LOS} is already calculated since the ground reflection can only occur when line-of-sight is present.

The factor $\Gamma_{\|}$ is present since there is a reflection on the ground and since the polarisation of the electric field from the base station is parallel to the plane of incidence and is equal to

$$\Gamma_{\|} = \frac{cos\theta_i - \frac{1}{\sqrt{\epsilon_r}}\sqrt{1 - \frac{1}{\epsilon_r}sin^2\theta_i}}{cos\theta_i + \frac{1}{\sqrt{\epsilon_r}}\sqrt{1 - \frac{1}{\epsilon_r}sin^2\theta_i}} \tag{6}$$

The angle θ_i can be determined using

$$\begin{aligned} cos\theta_i &= \frac{2h_{bs}}{d^{GROUND}} \\ \Leftrightarrow \theta_i &= cos^{-1}(\frac{2h_{bs}}{d^{GROUND}}) \end{aligned} \tag{7}$$

Here again the property that both the base station and receiver are at the same height, is used.

Finally the effective height is determined using formula (2). Here is θ equal to θ_i calculated above. One then obtains that the open circuit voltage is equal to

$$\begin{aligned} V_{oc}^{GROUND} &= -\frac{\lambda}{\pi}\frac{cos(\frac{\pi}{2}cos(\theta))}{sin^2\theta}\vec{1_y} * \Gamma_{\|}\sqrt{60EIRP}\frac{e^{-j\beta d^{GROUND}}}{d^{GROUND}}\vec{1_\theta} \\ &= -\frac{\lambda}{\pi}\frac{cos(\frac{\pi}{2}cos(\theta))}{sin^2\theta}\Gamma_{\|}\sqrt{60EIRP}\frac{e^{-j\beta d^{GROUND}}}{d^{GROUND}}sin\theta \end{aligned} \tag{8}$$

3.3 Diffraction

Diffraction is calculated using following formula:

$$\vec{E}^{diff} = F(\upsilon)\sqrt{60EIRP}\frac{e^{-j\beta d^{LOS}}}{d^{LOS}}\vec{1_\theta} \tag{9}$$

With

$$\begin{aligned} \upsilon &= \sqrt{\frac{2}{\pi}\beta\Delta r} \\ |F(\upsilon)|^2[dB] &= -6.9 - 20log(\sqrt{(\upsilon - 0.1)^2 + 1} + \upsilon - 0.1) \qquad (\upsilon > 0) \\ \angle F(\upsilon) &= -\frac{\pi}{4} - \frac{\pi}{2}\upsilon^2 \qquad (\upsilon > 1) \\ \Delta r &= d_{diff} - d^{LOS} \end{aligned} \tag{10}$$

d_{diff} is equal to the distance the diffracted ray travels from base station to the receiver and d^{LOS} the distance the line-of-sight ray would travel if no object was present that blocked the line-of-sight.

Using the above formulas, a formula for $F(\upsilon)$ is constructed:

$$F(\upsilon) = \sqrt{10^{-6.9-20log(\sqrt{(\upsilon-0.1)^2+1}+\upsilon-0.1)}} * e^{j-\frac{\pi}{4}-\frac{\pi}{2}\upsilon^2} \tag{11}$$

Using this and the formula for the effective height (2), one obtains the open circuit voltage:

$$V_{oc}^{diff} = \vec{E}^{diff} * \vec{h_e}(\theta, \phi) \tag{12}$$

Note that the effective height for diffraction is equal to the one for line-of-sight.

3.4 Single Reflection Of A Building

The single reflection is calculated using Image Theory. The antenna is mirrored on the wall where the reflection takes place. The formula for the received electrical field is equal to

$$\vec{E}^{refl} = \Gamma_{\perp}\sqrt{60EIRP}\frac{e^{-j\beta d^{refl}}}{d^{refl}}\vec{1_{\theta}} \tag{13}$$

With d^{refl} the distance the wave travels between the base station and receiver and can be calculated using Pythagoras with the positions of the mirrored base station and the receiver:

$$d^{refl} = \sqrt{|x_{mirrored\,bs} - x_{receiver}|^2 + |y_{mirrored\,bs} - y_{receiver}|^2} \tag{14}$$

$\Gamma_{\perp}$ is present because there is a reflection present where the plane of incidence is perpendicular to the polarisation of the electric field from the base station. It is equal to

$$\Gamma_{\perp} = \frac{cos\theta_i - \sqrt{\epsilon_r}\sqrt{1 - \frac{1}{\epsilon_r}sin^2\theta_i}}{cos\theta_i + \sqrt{\epsilon_r}\sqrt{1 - \frac{1}{\epsilon_r}sin^2\theta_i}} \tag{15}$$

θ_i is calculated using following formula for reflections on a wall parallel to the y-axis

$$\theta = tan^{-1}(\frac{|y_{mirrored\,bs} - y_{receiver}|}{|x_{mirrored\,bs} - x_{receiver}|}) \tag{16}$$

And for a wall parallel to the x-axis

$$\theta = tan^{-1}(\frac{|x_{mirrored\,bs} - x_{receiver}|}{|y_{mirrored\,bs} - y_{receiver}|}) \tag{17}$$

The open circuit voltage is then calculated with

$$V_{oc}^{refl} = \vec{E}^{refl} * \vec{h_e}(\theta, \phi) \tag{18}$$

Where the effective height is equal to the one in equation (2).

3.5 Double Reflection Of A Building

Double reflections are also calculated using Image Theory. One first mirrors the base station on the wall where the first reflection occurs and then on the wall where the second reflection occurs. One now obtains for the electric field

$$\vec{E}^{refl} = \Gamma_{1\perp}\Gamma_{2\perp}\sqrt{60EIRP}\frac{e^{-j\beta d^{refl}}}{d^{refl}}\vec{1_{\theta}} \tag{19}$$

d^{refl} is calculated using formula (14) where the position of the mirrored base station is now equal to the base station position obtained after the second mirroring. The same is true for θ_{i2} (the incident angle of the second reflection) where formula (16) or (17) used. θ_{i1} is obtained by exploiting the property that $\theta_{i1} = \theta_{i2}$ when the two walls, where the reflections occur, are parallel to each other and $\theta_{i1} = \frac{\pi}{2} - \theta_{i2}$ when the walls are perpendicular to each other. The open circuit voltage is then calculated with

$$V_{oc}^{refl} = \vec{E}^{refl} * \vec{h_e}(\theta, \phi) \tag{20}$$

Where the effective height is the same as in equation (2).

4 Validation Of The Simulation

The simulation is validated in a few different ways. First, all ray trace components are evaluated separately to ensure that no error was made when considering reflections from different walls, line-of-sight reach, ... All the heat maps of the received power for every ray trace component (line-of-sight, diffraction, ground reflection and reflection of buildings) can be found in section 8.1.

Secondly, most of the channel properties discussed in section 5 are compared to graphs, theory and data that can be found in the theory and exercises of this course to validate whether the obtained results match the expected ones. One can for example plot the received power from the base station to the opposite wall while only taking line-of-sight and ground reflections into account (figure 1) and validate that it matches the results obtained in the theory of this course.

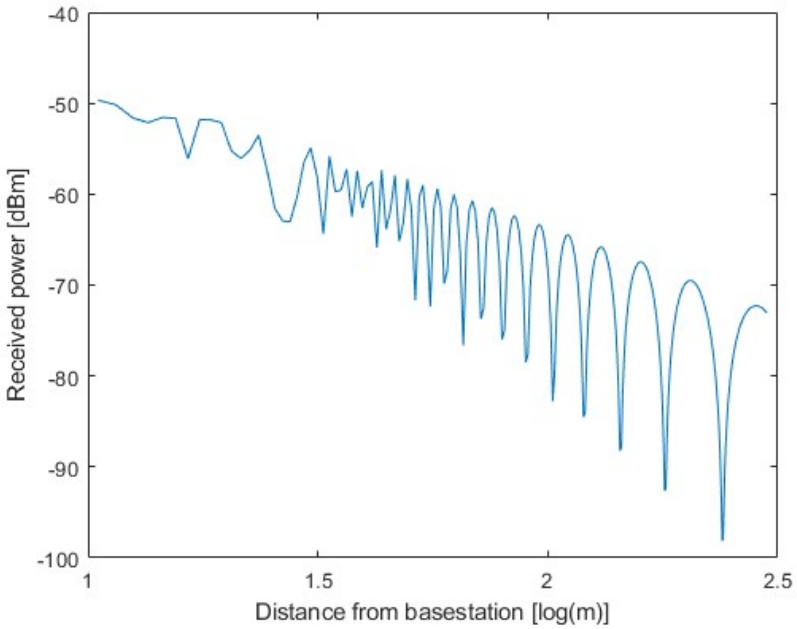

Figure 1: Received power from base station to the opposite wall with only line-of-sight and ground reflections taken into account

5 Channel Properties

This section discusses following channel properties: received power, signal-to-noise ratio, Rice factor, delay spread and the channel impulse response. For the first four properties a heatmap and a plot from the base station to the opposite wall of the property evaluated for the Marché aux Poissons is shown and discussed. The channel impulse response is evaluated at the intersections of the Marché with its side streets. A physical channel model and a tapped delay line where the bandwidth varies from narrow band to 200 MHz, is used to evaluate this.

5.1 Received Power

The received power is shown on figure 2. It is clear that there is interference present from reflections from the ground and walls. The received power is the highest close to the base station. This is expected since reflections cause a loss power and since the line-of-sight ray needs to propagate over a longer distance the further away from the base station. The received power when no reflections or line of sight is present, is significantly lower. This is due to the fact that diffraction causes a huge power loss. So it is clear to see that the receiver in the bottom streets has lower received power, compared to a receiver close to the base station. One can deduce from the graph on the right, that the received power can be approximated with a linear path loss. This is done in section 6.1.

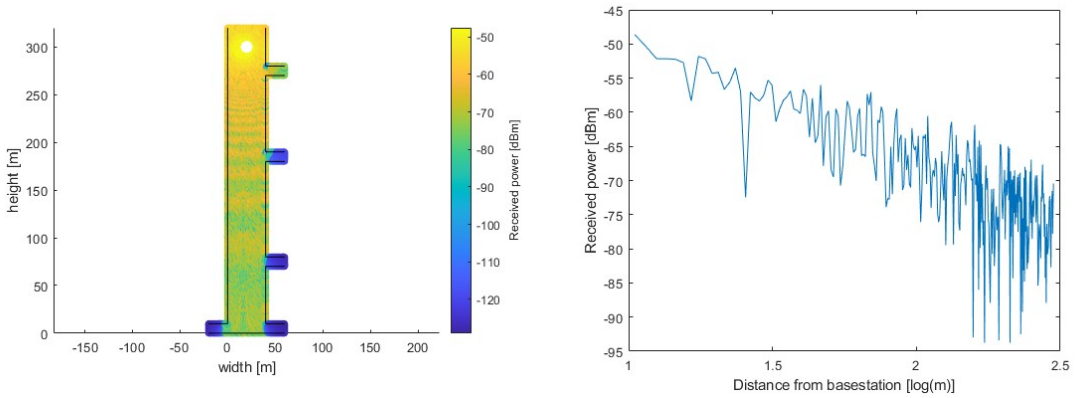

(a) Heatmap

(b) Between base station and opposite wall

Figure 2: Received power

5.2 Signal-to-noise Ratio

The signal-to-noise ratio is determined by dividing the received power by the noise power at the receiver. The noise consists in this case of two parts: the receiver noise figure and the thermal noise. The receiver noise figure is given by the channel parameters and is equal to 15 dB. The thermal noise power is calculated using following formula:

$$\begin{aligned} P_{thermal\,noise}[dB] &= 10 * log(kT_0BW) \\ &= 10 * log(1.379 * 10^{-23} \frac{W}{Hz * K} * 293K * 200 * 10^6 Hz) \\ &= -90.925\,dB \end{aligned} \tag{21}$$

Where BW is the bandwidth equal to 200 MHz, k the Boltsmann constant and T_0 the absolute temperature in Kelvin.

If one subtracts the noise components from the received power, the signal-to-noise ratio is obtained:

$$SNR[dB] = P_{received}[dB] - P_{noise\,figure}[dB] - P_{thermal,noise}[dB] \tag{22}$$

The signal-to-noise ratio is shown in figure 3. Since it is equal to the received power minus the total noise power, that is constant, the same results as the received power, but shifted, are observed. So here the same conclusions as for the received power can be made. Close the base station, a high signal-to-noise ratio can be observed, the further away, the lower the signal-to-noise ratio (figure 3b). There is interference present that causes variation in the signal-to noise ratio. Where there is only diffraction present, the signal-to-noise ratio, drops to very low values.

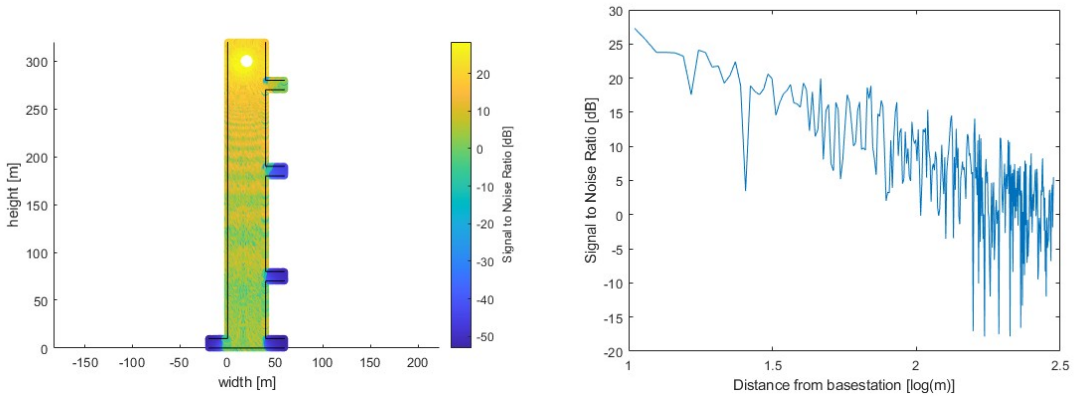

(a) Heatmap

(b) Between base station and opposite wall

Figure 3: Signal-to-noise ratio

5.3 Rice factor

The rice factor K compares the power of the line-of-sight wave (a_0^2), with the mean power of the multipath waves (a_n^2) and is given by following formula:

$$K[dB] = 10 * log \frac{a_0^2}{\sum_{n=1}^{N} a_n^2} \tag{23}$$

The Rice factor for the simulation is shown in figure 4. One can observe that the Rice factor is the highest close to the base station. This can be explained by the fact that close to the base station, the received power from the line-of-sight component is large and that the travelled distance of the reflected waves, especially those that reflect on the bottom wall, is also rather large. This causes a low received power from the reflected waves.

Moving closer to the bottom wall and away from the base station reduces the rice factor. This is caused by the line-of-sight wave increasing in length while the length of the reflected waves from the bottom wall decreases. The length of the waves from the reflections from the left and right walls approach the length of the line-of-sight wave. This means that the received power from the reflected waves from the left and right wall come close to the received power from the line-of-sight wave while the received power from reflections from the bottom wall increases (the received power from the reflections from the bottom wall can be seen in figures 12c, 13f, 14a, 13b, 13e).

The figure also shows lines originating from the side streets. These lines are areas with a higher Rice factor. This higher Rice factor is caused by the absence of a reflected wave coming from the right walls where the streets are located, since the streets interrupt the walls and thus no reflection is possible there, this causes a lower $\sum_{n=1}^{N} a_n^2$. This can also be clearly seen on figure 4b.

For areas where no line-of-sight present, the Rice factor is equal to zero or $-\infty$ dBm since a_0 is equal to 0.

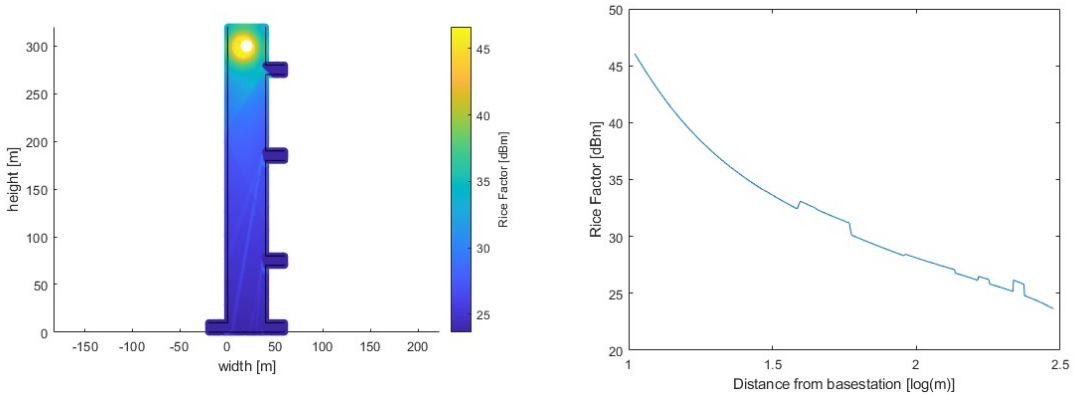

(a) Heatmap

(b) Between base station and opposite wall

Figure 4: Rice factor

5.4 Delay Spread

The delay spread is the difference in time between when the first wave arrives and when the last wave arrives at the receiver and is shown in figure 5.

The delay spread is the highest around the base station. This is caused by the reflections of the waves with the bottom wall and the proximity of the base station to the receiver. The time of arrival of the line-of-sight wave around the base station is very low and the time of arrival of the waves reflected on the bottom wall is rather high. This is easily explained by the fact that the travel time from base station to receiver is proportional to the length of the path the wave travels. So the arrival of the wave at the receiver is later in time for waves that travel a longer distance, in this case especially true for waves that reflect from the bottom wall. The line-of-sight wave on the other hand travels a short distance and arrives thus way quicker at the receiver. At the bottom wall, the delay spread is low, since the travelled distance of the waves are closer to each other. So the time of arrival of each wave will be closer to each other and thus creating a much lower delay spread.

The streets all have a low delay spread, since reflections from the bottom wall can only reach for a small amount into the streets (figures 12c, 13f, 14a, 13b, 13e, 14b). This eliminates the large delay from reflections from the bottom wall, especially for streets closer to the base station. Receiver positions where only a diffracted ray arrives, have of course a delay spread of zero since only one wave arrives.

Finally, a linear relation between the delay spread and distance from the base station for a receiver moving between the base station and bottom wall can be observed in figure 5b. Note that the distance is given in m and not log(m) to emphasize the linear relation. The linear relationship is caused by the geometry of the walls. The wave with the largest total travel distance, and thus largest delay, can reflect over the whole length of the left and bottom wall since there are no streets present in those walls (except for the bottom of the left wall, but this can be neglected). The line-of-sight wave is always present between the base station and bottom wall and is the fastest wave that arrives at the receiver. These two waves define the delay spread and thus the linearity.

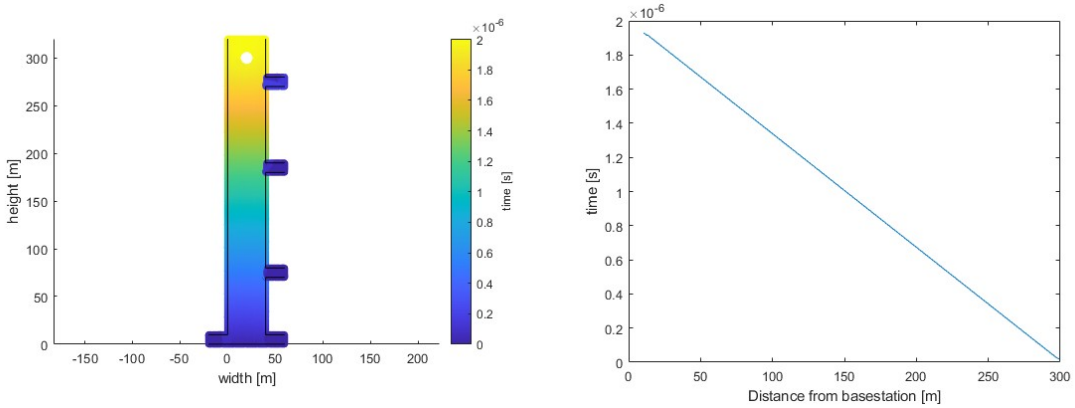

(a) Heatmap

(b) Between base station and opposite wall

Figure 5: Delay spread

5.5 Channel Impulse Response

The fysical channel impulse response is calculated by taking the open circuit voltage at the receiver V_{oc} of each wave and dividing it by the voltage at the transmitter:

$$h = \frac{V_{oc}}{V_{tx}} = \frac{\sqrt{\frac{1}{8R_a}}V_{oc}}{\sqrt{\frac{EIRP}{G(\theta)}}} \tag{24}$$

With $G(\theta) = \frac{16}{3\pi}sin^3(\theta)$ the gain of the transmitter antenna and R_a the transmitter antenna impedance. The delay is calculated using $\tau = \frac{r}{c}$. With r the distance the wave travels and c the speed of light.

The channel responses for the tapped delay line are calculated by summing the impulses that arrive in the same tap. The tap width $\Delta\tau$ is equal to $\frac{1}{\frac{1}{2}BW}$. The band width varies from narrow band to 2000 MHz. Note that uncorrelated scattering is assumed.

The physical channel impulse response is given for the five intersections with the side streets and are given in figure 6. One can see that the impulse response is more spread out for a receiver at an intersection close to the base station then for a receiver closer to the bottom wall. One can also see that in general the impulse amplitude is lower for waves that arrive later in time at the intersection. This is especially the case for the intersections closer to the base station. Both these effects can be explained by the long distance the waves, that reflect from the bottom wall, travel. Closer to the bottom wall, the impulses have a more equal amplitude and arrive at the receiver closer to each other in time. These waves are also visualised in figure 7.

The bandwidth of the tapped delay line channel influences the amount of impulses and their amplitude the receiver receives. A narrow band channel receives only one impulse, while a channel with a large bandwidth receives all the impulses separately and is almost equivalent to the physical channel impulse response. For channels with a small bandwidth, the pulses in one tap are added to each other. This can cause destructive interference and can result in a lower impulse amplitude compared to the wide band channel. But the opposite effect can also be true, constructive interference can occur and can result in a higher impulse for the channel with low band width.

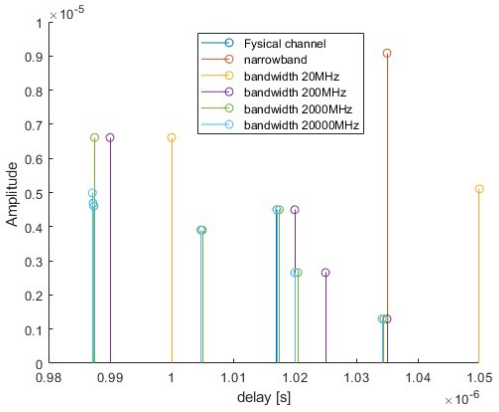

(a) Intersection With Pl. Sainte-Catherine on the right

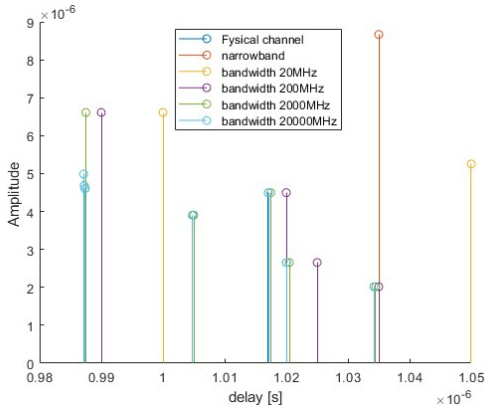

(b) Intersection With Pl. Sainte-Catherine on the left

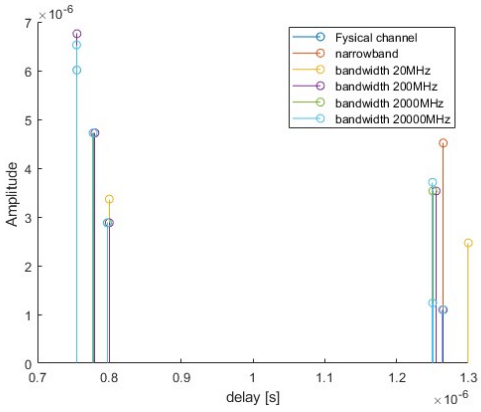

(c) Intersection With Rue Du Peuplier

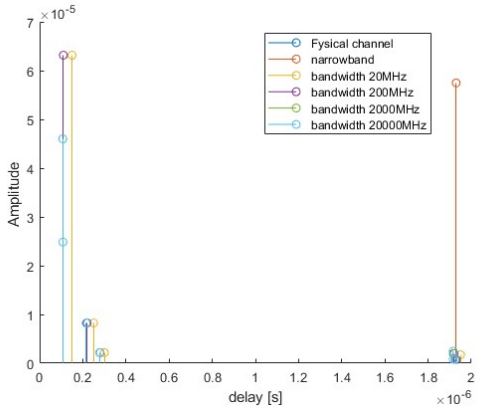

(d) Intersection With Rue Du Grand Hospice

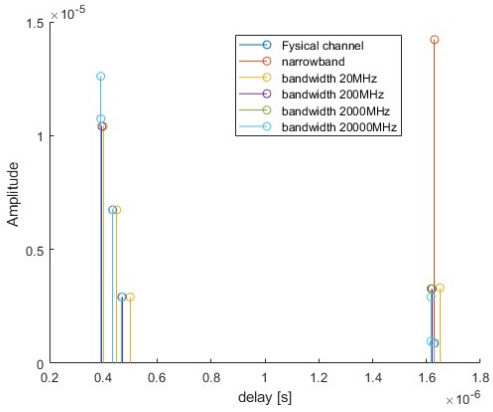

(e) Intersection With Rue Du Rouleau

Figure 6: Impulse response amplitudes at each of the intersections

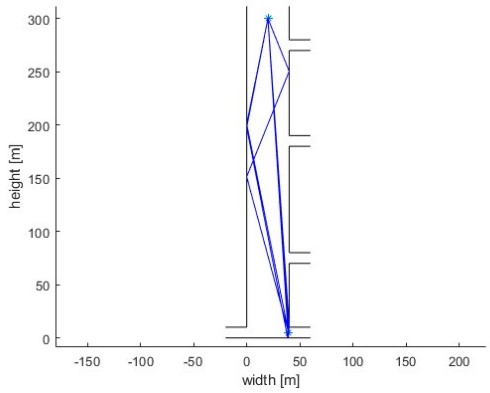

(a) Intersection With Pl. Sainte-Catherine on the right

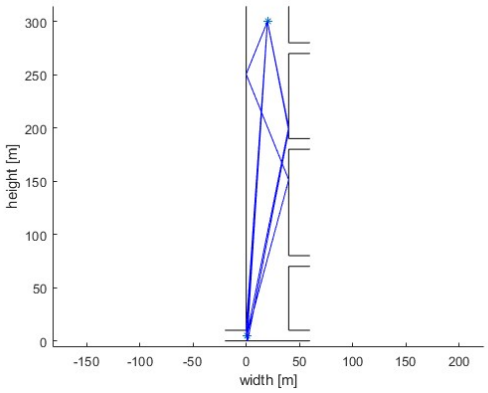

(b) Intersection With Pl. Sainte-Catherine on the left

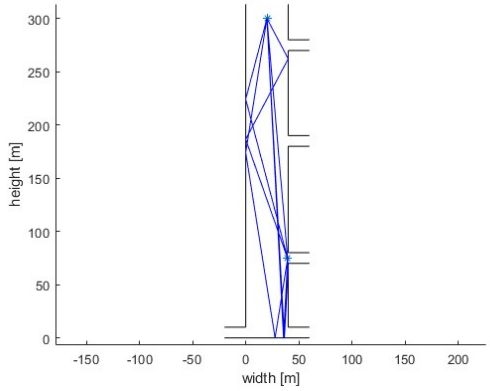

(c) Intersection With Rue Du Peuplier

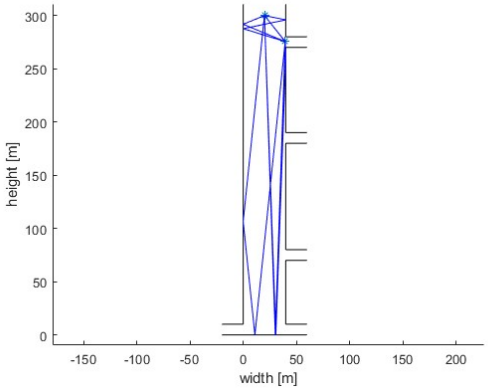

(d) Intersection With Rue Du Grand Hospice

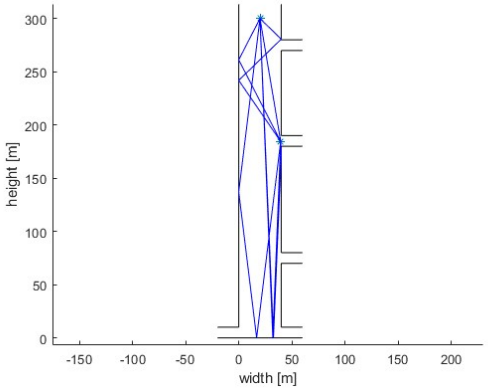

(e) Intersection With Rue Du Rouleau

Figure 7: Traced rays at each of the intersections

6 Propagation Model

6.1 Path Loss

The path loss of the channel is determined between the base station and the opposite wall. This is done by the use of linear regression in the log domain. Figure 8 shows the obtained curve compared to the simulated channel received power. The choice for linear regression with one curve is easily made, since one can assume that the obtained results from the simulation are similar to those of an urban canyon model. From figure 8 one can deduce that the path loss is equal to around -19 $\frac{dBm}{log(m)}$.

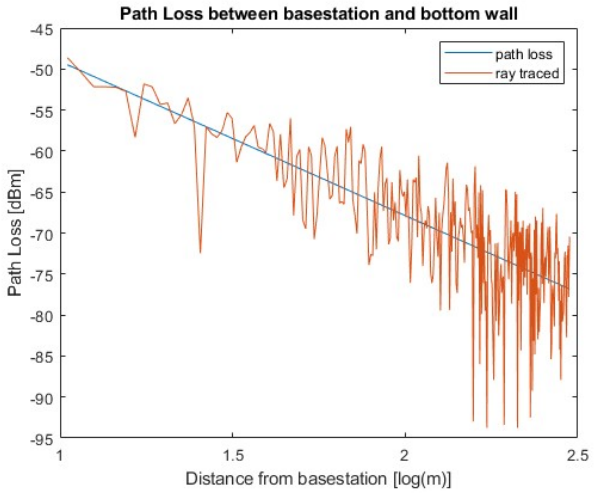

Figure 8: Obtained path loss model plotted together with simulated received power

6.2 Statistical Fading Characterisation

The statistical fading is characterised by calculating the variance of the simulated received power with the path loss obtained in the previous section. The results are shown in figure 9a. The distribution that looks the most fitting is the log-normal distribution and is also shown in the figure. It looks like a normal distribution since the variance is determined in the log domain. The obtained variance is then equal to 29.5810 $\frac{dBm}{log(m)}$.

The results of the model using the path loss and statistical fading can be seen in figure 9b, where the curve is determined by adding a random normal distributed variable with zero mean and a variance equal to the one obtained above, to the path loss.

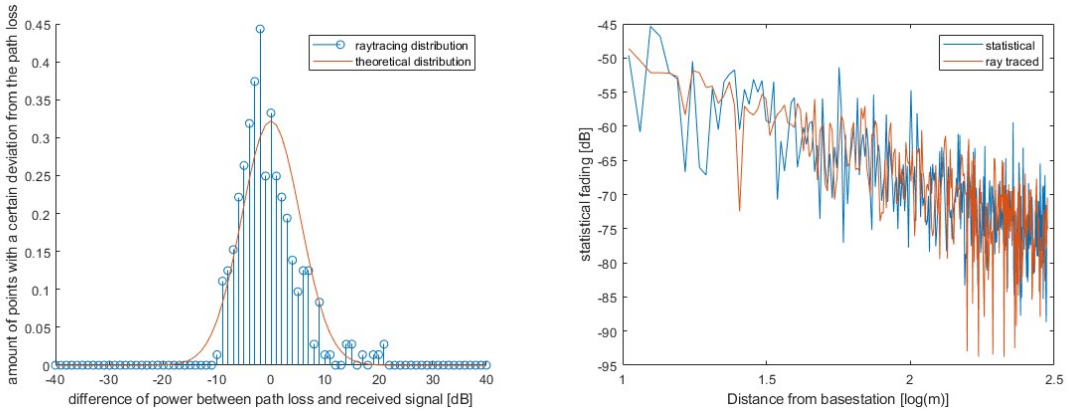

(a) theoretical and simulated variance

(b) Statistical fading vs simulated received power

Figure 9: Statistical fading

6.3 Cell Range

The cell range as a function of the connection probability at the edge is determined by calculating the maximal path loss L_{max}. This path loss is equal, except in sign, to the minimal received power P_{min} since the EIRP of the transmitter is equal to 0 dB. Using this minimal received power and the path loss model, the maximal distance d^{max} is calculated. The formulas are given below:

$$\begin{aligned} \gamma[dB] &= erfc^{-1}(2(1-p_{connection})\sqrt{2}\sigma_L) \\ L_{max}[dB] &= -P_{thermal\,noise}[dB] - P_{noise\,figure}[dB] - SNR_{target} - \gamma \\ P_{min}[dB] &= -L_{max}[dB] \\ d^{max} &= 10^{\frac{P_{min} - intercept_{path\,loss}}{slope_{path\,loss}}}[m] \end{aligned} \tag{25}$$

Where γ the fade margin, $p_{connection}$ the probability of connection at the cell edge, σ_L^2 the variance of the statistical fading, SNR_{target} the wanted signal-to-noise level at the receiver (here 5 dB), $intercept_{path\,loss}$ the Y intercept and $slope_{path\,loss}$ the slope of the path loss model.

The obtained results are shown in figure 10. For a connection probability smaller then 14%, the base station cell range suffices for the whole length of the Marché aux Poissons. But for higher connection probabilities, the cell range drops drastically. The cell range for a connection probability of 99%, is only 31 meters.

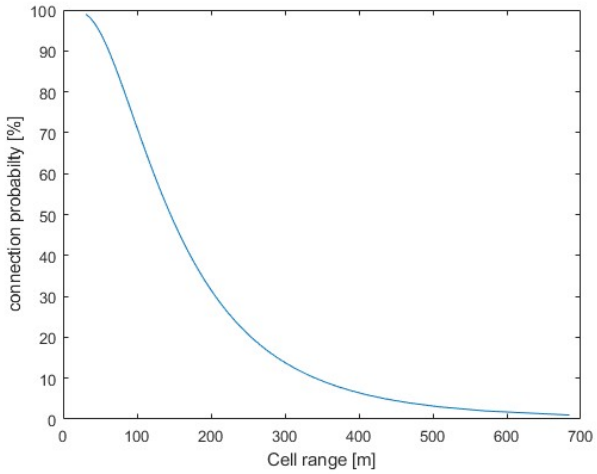

Figure 10: Cell range as a function of the connection probability at the cell edge

7 Conclusion

The modeling of a channel is a quite complicated process. One has to take many things into account ranging from reflections to noise figures at the receiver. The simulation has made it clear that the environment of the channel has a huge impact on the channel properties.

The obtained path loss model with statistical fading shows that the connection probability at the cell edge has an influence on the cell range. If a connection probability of 14% suffices at the bottom wall, then the current base station has enough power. But for higher connection probabilities at the bottom wall, a base station with a higher EIRP, or an extra base station closer to the bottom wall should be placed.

8 Appendix

8.1 Evaluation Of All Ray Trace Components

Below are the heatmaps for every considered ray used to model the Marché aux Poissons.

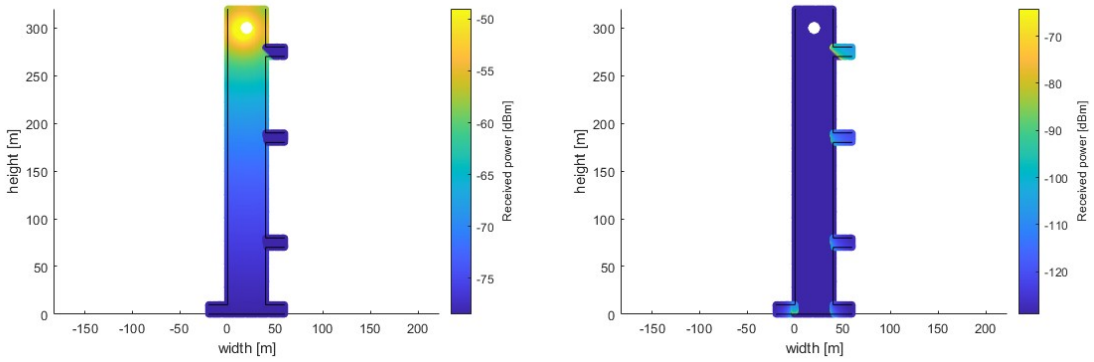

(a) Line-of-sight

(b) Diffraction

Figure 11: Received power only considering Line-of-sight and diffraction rays

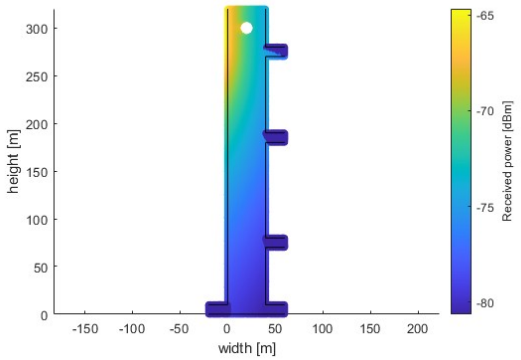

(a) Left wall

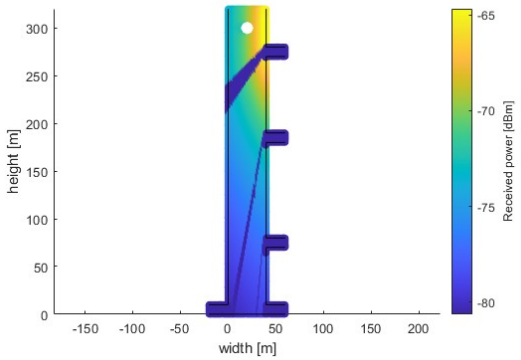

(b) Right wall

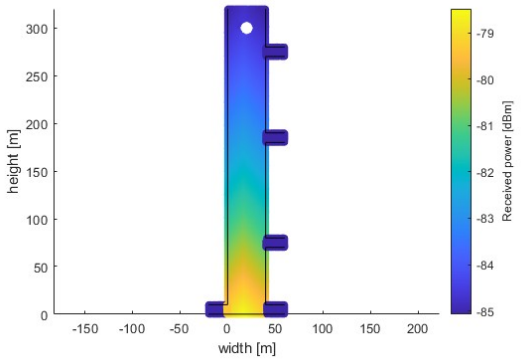

(c) Bottom Wall

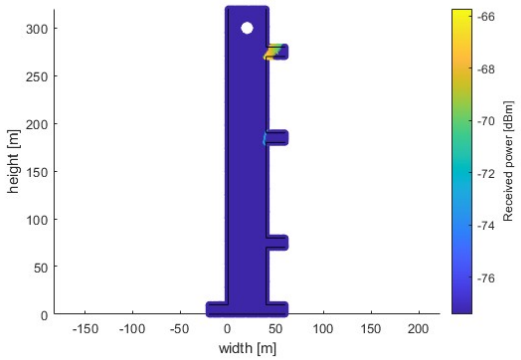

(d) Streets

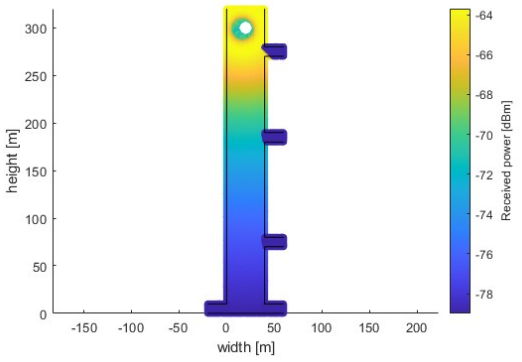

(e) Ground

Figure 12: Received power only considering single reflection rays

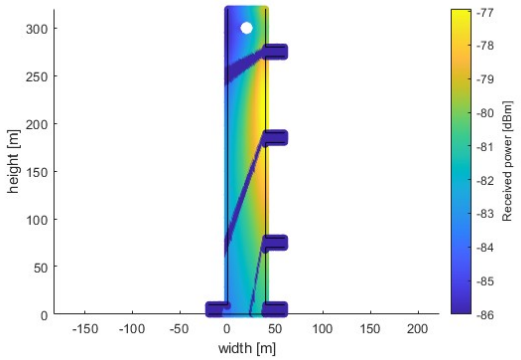

(a) Left wall and right wall

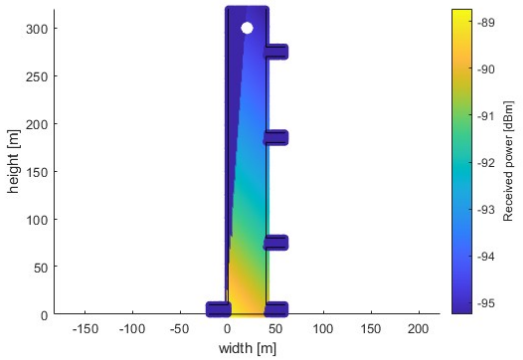

(b) Left wall and bottom wall

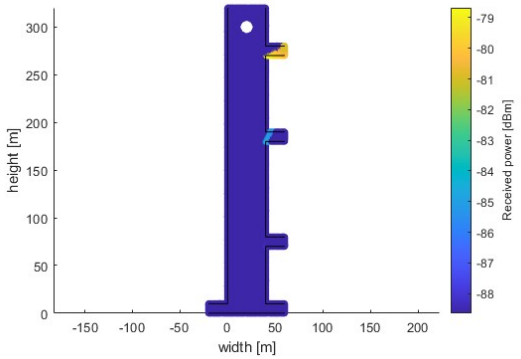

(c) Left wall and streets

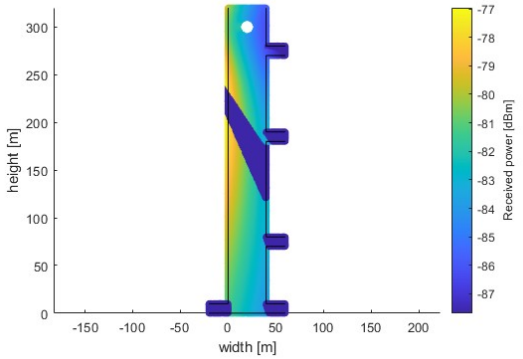

(d) Right wall and left wall

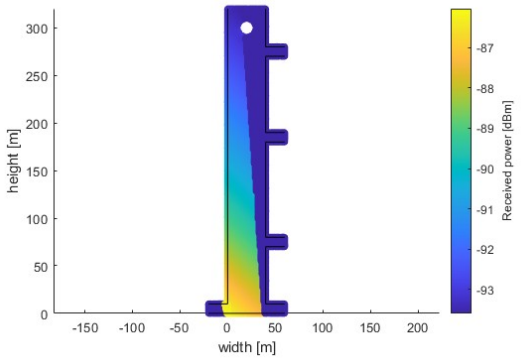

(e) Right wall and bottom wall

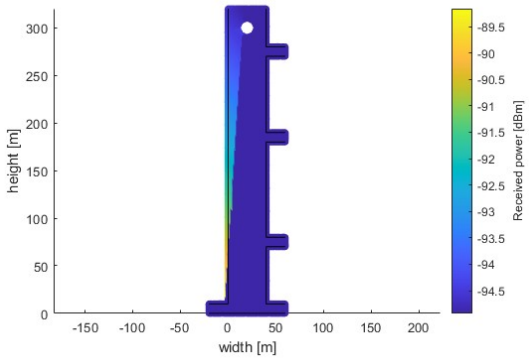

(f) Bottom wall and left wall

Figure 13: Received power only considering double reflection rays (part 1)

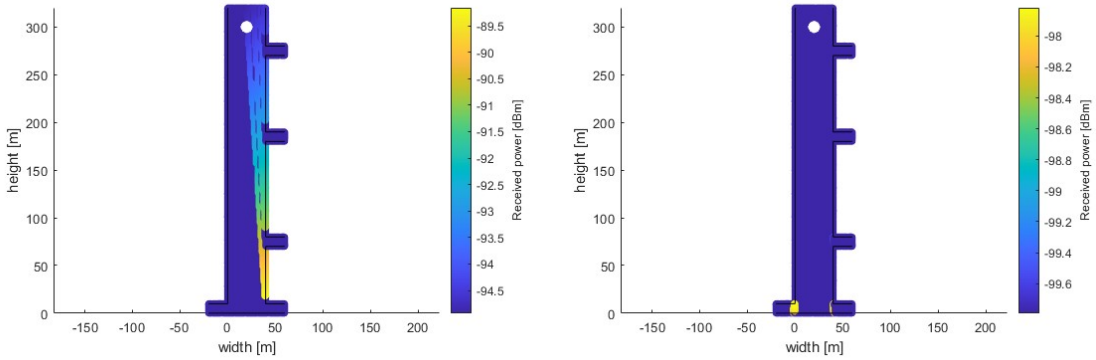

(a) Bottom wall and right wall

(b) Bottom wall and streets

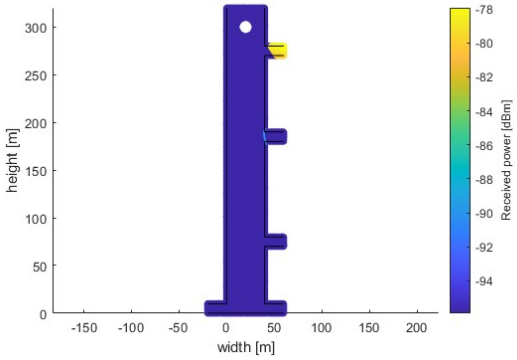

Figure 14: Received power only considering double reflection rays (part 2)